AGU PUBLICATIONS

JGR

Journal of Geophysical Research: Space Physics

RESEARCH ARTICLE

10.1002/2016JA022498

Key Points:

- Oxygen ions do not follow the protons in bursty bulk flows, they move much slower
- Oxygen ions are less accelerated in the plasma sheet than protons
- The earthward transport of oxygen is slower than for protons

Correspondence to:
H. Nilsson,
hans.nilsson@irf.se

Citation:
Nilsson, H., M. Hamrin, T. Pitkänen, T. Karlsson, R. Slapak, L. Andersson, H. Gunell, A. Schillings, and A. Vaivads (2016), Oxygen ion response to proton bursty bulk flows, *J. Geophys. Res. Space Physics*, *121*, 7535–7546, doi:10.1002/2016JA022498.

Received 5 FEB 2016
Accepted 22 JUL 2016
Accepted article online 28 JUL 2016
Published online 9 AUG 2016

Oxygen ion response to proton bursty bulk flows

Hans Nilsson[1,2], Maria Hamrin[3], Timo Pitkänen[3], Tomas Karlsson[4], Rikard Slapak[2], Laila Andersson[5], Herbert Gunell[6], Audrey Schillings[1,2], and Andris Vaivads[7]

[1]Swedish Institute of Space Physics, Kiruna, Sweden, [2]Division of Space Technology, Luleå University of Technology, Kiruna, Sweden, [3]Department of Physics, Umeå University, Umeå, Sweden, [4]Space and Plasma Physics, School of Electrical Engineering, Royal Institute of Technology, Stockholm, Sweden, [5]Laboratory for Atmospheric and Space Physics, Boulder, Colorado, USA, [6]Royal Belgian Institute for Space Aeronomy, Brussels, Belgium, [7]Swedish Institute of Space Physics, Uppsala, Sweden

Abstract We have used Cluster spacecraft data from the years 2001 to 2005 to study how oxygen ions respond to bursty bulk flows (BBFs) as identified from proton data. We here define bursty bulk flows as periods of proton perpendicular velocities more than 100 km/s and a peak perpendicular velocity in the structure of more than 200 km/s, observed in a region with plasma beta above 1 in the near-Earth central tail region. We find that during proton BBFs only a minor increase in the O^+ velocity is seen. The different behavior of the two ion species is further shown by statistics of H^+ and O^+ flow also outside BBFs: For perpendicular earthward velocities of H^+ above about 100 km/s, the O^+ perpendicular velocity is consistently lower, most commonly being a few tens of kilometers per second earthward. In summary, O^+ ions in the plasma sheet experience less acceleration than H^+ ions and are not fully frozen in to the magnetic field. Therefore, H^+ and O^+ motion is decoupled, and O^+ ions have a slower earthward motion. This is particularly clear during BBFs. This may add further to the increased relative abundance of O^+ ions in the plasma sheet during magnetic storms. The data indicate that O^+ is typically less accelerated in association with plasma sheet *X* lines as compared to H^+.

1. Introduction

Ionospheric-origin oxygen ions play an important part in the dynamics of the Earth's magnetosphere. The full chain of ion circulation involves ionospheric upflow, subsequent magnetospheric energization, and finally transport through the magnetosphere to some final destination. One important destination for the outflow is escape from the Earth's magnetosphere, either directly to the magnetosheath [*Slapak et al.*, 2013] or through the distant tail. Another important destination is the plasma sheet with a subsequent transport back toward Earth [*Seki et al.*, 2001]. *Kronberg et al.* [2014] provide a thorough review of the transport and energization of O^+ in the Earth's magnetosphere. The aim of this study is to look at the transport of O^+ in the plasma sheet back toward Earth in association with bursty bulk flows (BBFs).

The ionospheric cusp is the main source of oxygen ions observed over the polar cap, in the mantle, and in the magnetosheath [*Dubouloz et al.*, 2001; *Nilsson et al.*, 2012; *Slapak et al.*, 2013]. Oxygen ions in the lobes are frequently believed to be of cusp origin. Transport of O^+ through the tail lobes toward the plasma sheet has been studied in detail [*Liao et al.*, 2010, 2012]. It has been shown how the flux of O^+ is modulated by the solar cycle and geomagnetic activity [*Kistler et al.*, 2006; *Mouikis et al.*, 2010; *Kistler et al.*, 2010; *Maggiolo and Kistler*, 2014]. The transport of plasma toward the plasma sheet is faster for high geomagnetic activity, leading to higher O^+ plasma sheet densities for disturbed conditions. Much less is known about the flow of O^+ back toward Earth. *Ohtani et al.* [2015] studied the energy density ratio of O^+ and H^+ in relation to fast flows using Geotail data. They found that the O^+ to H^+ energy density ratio decreased with faster earthward flow whereas it increased with faster tailward flow.

As a consequence of reconnection, plasma earthward of a neutral line (*X* line) in the plasma sheet is transported toward Earth. If frozen-in conditions hold for both H^+ and O^+, the two ions species should have the same transport pattern perpendicular to the magnetic field. The velocity along the field line may also be similar, as H^+ and O^+ in the mantle and lobes are often observed to have the same velocity [*Nilsson et al.*, 2006]. If ions are accelerated in a finite region (i.e., near an *X* line), the velocity filter effect may cause all ions observed at some distance from the source to have a similar velocity [e.g., *Dubouloz et al.*, 2001; *Nilsson et al.*, 2004; *Liao et al.*, 2010].

The earthward velocity is thus determined either by the general earthward convection or by how the two ion species are accelerated in the vicinity of the reconnection site where earthward flow is initiated. *Shay and Swisdak* [2004] have shown that the addition of a heavy minor ion species (i.e., O^+) modifies the outer reconnection region where ions are accelerated. The results presented by *Shay and Swisdak* [2004] indicate that O^+ will be less accelerated and may also slow the total reconnection rate. Similarly, *Liu et al.* [2015] performed 2.5-D particle-in-cell simulations and found that O^+ was demagnetized in a larger region than H^+, the heavy ion diffusion region. They also found that O^+ was energized by both the *x* and *y* components of the electric field, while H^+ was mainly energized by the *x* component.

Transient reconnection leads to bursts of accelerated ions. The associated transient increases in the earthward flow of plasma, known as BBFs, play an important role in the earthward transport of plasma [*Angelopoulos et al.*, 1994]. BBFs are defined as regions with strongly enhanced earthward proton flows. For statistical studies some more rigorous definition is needed, even though the precise definition is somewhat arbitrary. In the work of *Angelopoulos et al.* [1994] BBFs were defined as periods with earthward flows above 100 km/s, with a peak magnitude within the structure of at least 400 km/s. *Pitkänen et al.* [2013] used a criterion of a convective (magnetic field perpendicular) flow velocity in the $X_{GSM} - Y_{GSM}$ plane above 200 km/s.

Model results like *Ge et al.* [2011] show that the scale size of features like bursty bulk flows may be of the order of magnitude of the O^+ ion gyroradius. O^+ ions may thus not behave as frozen in to such structures. *Kistler et al.* [2005] have shown examples of this different behavior of H^+ and O^+ in thin current sheets, with the O^+ moving along the tail duskward electric field while the protons mainly drift earthward. This indicates that O^+ may be energized by the motion along the electric field, but may also move out of a spatially limited flow region, rather than drift along with the protons.

Given the larger gyroradius of oxygen ions (for the same energy), it is not obvious that oxygen will be transported in a similar way as protons in the plasma sheet in general. This is even more true for bursty bulk flows, which are of limited spatial and temporal extent. Indeed, a visual inspection of bursty bulk flow data used in other studies [*Pitkänen et al.*, 2013; *Hamrin et al.*, 2014] shows that frequently the O^+ ions do not appear to be much accelerated at all at the time of peak H^+ velocity. On the other hand, *Zong et al.* [2008] showed cases of O^+-dominated bursty bulk flows, observed during storm times when the O^+ number density exceeded the H^+ number density by a factor of 3 to 5. For that situation the velocities of H^+ and O^+ were fairly similar (reaching about 400 km/s and 600 km/s, respectively), so this does happen for some circumstances. There are also reports of O^+ flow in the distant tail which is apparently associated with reconnection in the tail [*Zong et al.*, 1998]. A statistical study of high-energy O^+ ions (140 keV–1 MeV) indicated strong acceleration of O^+ associated with near-Earth reconnection [*Luo et al.*, 2014]. *Greco et al.* [2015] reported test particle simulations of O^+ response to dipolarization fronts (which are associated with BBFs). They found that they could reproduce a high-energy tail similar to what was reported by *Luo et al.* [2014] and also that for the bulk of the population the O^+ ions were not accelerated to the same velocity as were H^+.

Thus, O^+ ions may both be less accelerated than H^+ in the region of ion acceleration and behave in a different way within the enhanced flow region. The behavior of O^+ in response to BBFs is the subject of this study where we show both how O^+ is transported in the plasma sheet and how it responds to reconnection as compared to the much more studied H^+ population.

2. Method

2.1. Data Set

Ion and magnetic field data from the Cluster spacecraft [*Escoubet et al.*, 2001] from the years 2001 to 2005 have been used in this study. This corresponds to the declining phase of a solar cycle 23.

The ion data were obtained with the mass resolving CODIF instrument on spacecraft 4 [*Rème et al.*, 2001]. CODIF data from the high sensitive magnetosphere modes were used. The energy interval used was 40 eV to 40 keV. CODIF bins data into four mass ranges, H^+, He^{2+}, He^+, and O^+. Here only H^+ and O^+ data were used. CODIF obtains one full distribution function every 4 s spin, but the downlinked data may be of 4 to 12 s resolution. The ion data were combined with magnetic field estimates obtained from the Cluster fluxgate magnetometer [*Balogh et al.*, 2001]. Throughout this study 4 s spin-averaged magnetic field data were used.

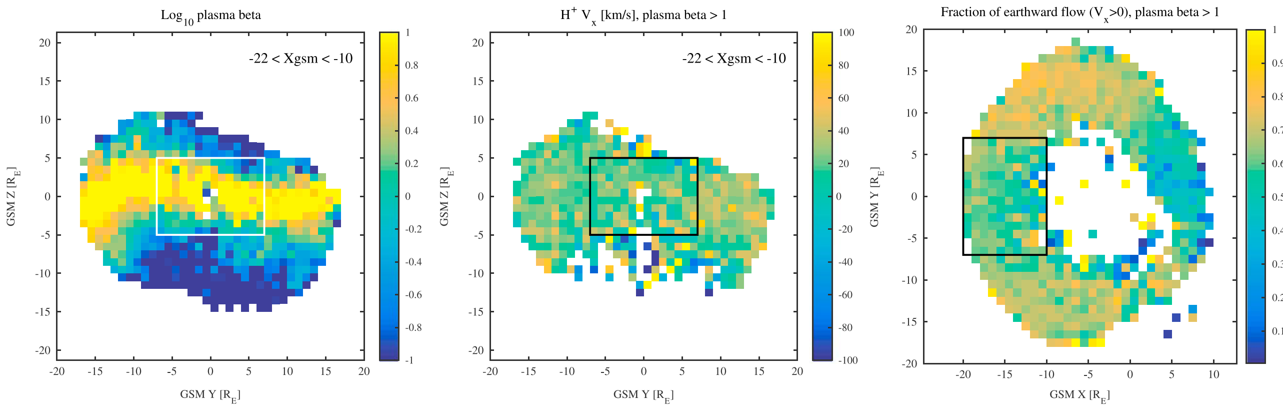

Figure 1. Illustration of (left) the average plasma beta in the $Y_{GSM} - Z_{GSM}$ plane averaged over the region $X_{GSM} < -10\ R_E$ and (middle) the average earthward H^+ motion for cases with plasma beta >1. (right) The occurrence frequency for earthward motion for plasma beta >1 in the $X_{GSM} - Y_{GSM}$ plane. The spatial region of the selection criteria is indicated with a white box in Figure 1 (left), and with black boxes in the other panels.

Integrated moment data were used, which may have to be taken into consideration as the ion distributions are frequently not Maxwellian, see discussion in section 3.2.

In this study, data were removed when there was an indication that H^+ fluxes could have influenced the O^+ measurements, as discussed by *Nilsson et al.* [2006]. In practice, this affects only a small part of the data outside the cusp/mantle and magnetosheath, due to less intense proton fluxes.

Another potential problem when comparing different ion species is the limited energy range of the instrument. Bursty bulk flows may reach velocities of 1000 km/s for H^+. This velocity is outside the instrument measurement range for O^+. If O^+ is accelerated to the same velocity as H^+, the bulk of the O^+ population would be outside the instrument measurement range. This is further discussed in section 4.

2.2. Data Selection Criteria

In order to study the flow in the plasma sheet a similar criterion for identification of the plasma sheet, as in a series of previous papers, has been used [*Kistler et al.*, 2006; *Mouikis et al.*, 2010; *Kistler et al.*, 2010; *Maggiolo and Kistler*, 2014]: The plasma beta must be above 1, the position $X_{GSM} < -10$ Earth radii (R_E), $|Y_{GSM}| < 7\ R_E$, and $|Z_{GSM}| < 5\ R_E$. Finally, the proton density N_H must be less than 2 cm^{-3}. Both tailward and earthward flows are accepted. A criterion to remove any possible magnetosheath data has also been implemented, by demanding that $T_\perp$ (eV) N_H (cm^{-3}) > 1000 [*Hamrin et al.*, 2009], as higher temperatures and lower densities are expected in the plasma sheet as compared to the magnetosheath [*Hamrin et al.*, 2009]. In order to have meaningful velocity estimates a lower limit is also set on the minimum ion density for both H^+ and O^+. Both 10^{-2} cm^{-3} and 10^{-3} cm^{-3} were tested. The former reduced the number of BBFs in the superposed epoch analysis significantly while otherwise giving qualitatively similar results. A density threshold of 10^{-3} cm^{-3} as lower density limit was therefore chosen for the data used in this study.

The region studied is illustrated in Figure 1. The spatial region of the selection criteria is indicated with a white box in Figure 1 (left) and with black boxes in the other panels.

Figure 1 (left) shows the plasma beta between X_{GSM} $-10\ R_E$ and $-20\ R_E$. Figure 1 (middle) shows the earthward flow velocity of H^+ for data points with plasma beta >1. The average flow is earthward (positive) throughout the measurement region. Figure 1 (right) shows the relative occurrence of earthward flows for data points with plasma beta >1. Earthward flows dominate, in particular, at the flanks outside our spatial selection criteria. This indicates that the spatial selection criteria do not significantly influence the results but also that the flank regions may require a separate study.

For plasma transport to and from the tail the total earthward velocity is of interest (i.e., the V_x component). In the plasma sheet the plasma beta is unity or higher, so that it may be that the magnetic field lines are carried by the plasma flow rather than guiding it. The magnetic field may also exhibit fast variations, which may pose a problem when calculating velocity moments in a magnetic field reference frame. For studies of plasma dynamics the corresponding magnetic field perpendicular component $V_{\perp x}$ is still of particular interest as it reflects the plasma convection, and should to first order be the same for all ion species (assuming frozen-in conditions hold).

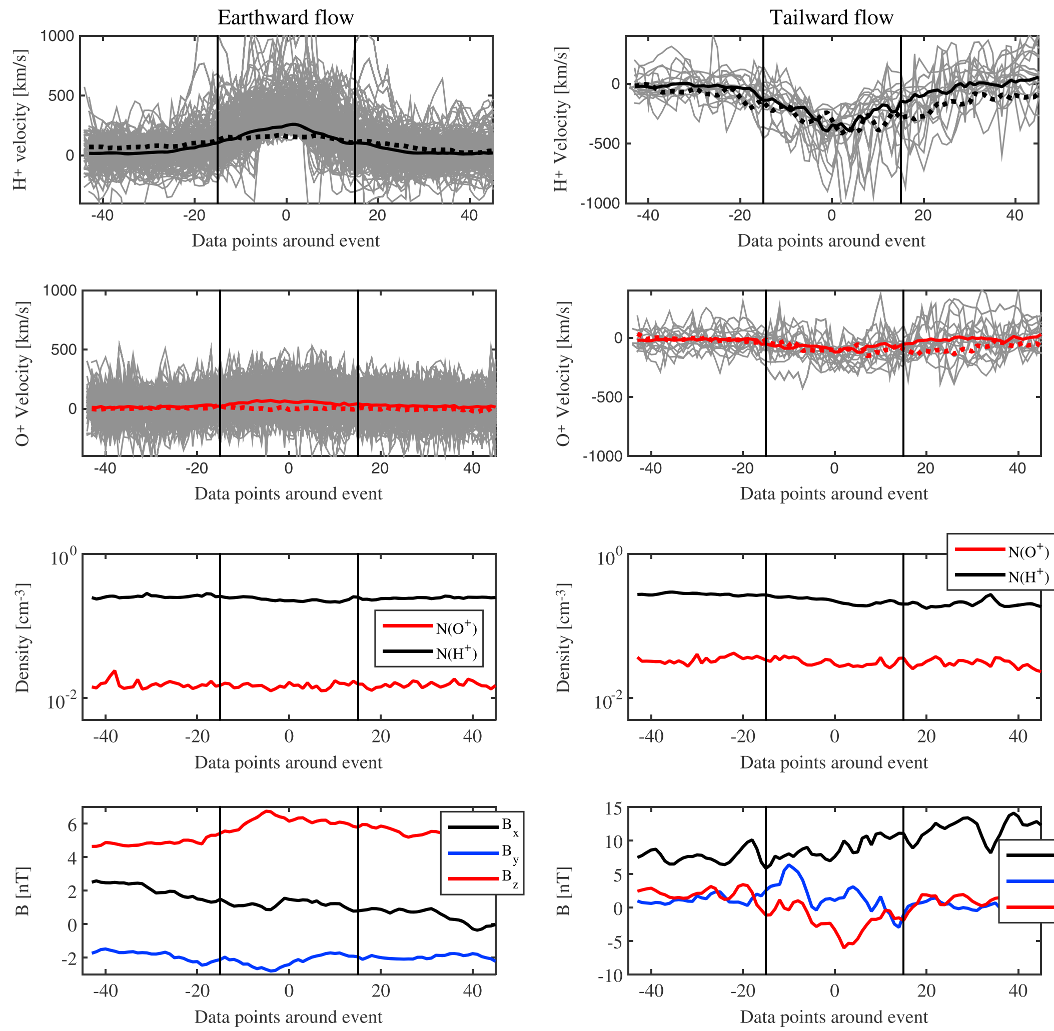

Figure 2. Superposed epoch analysis of (left) earthward and (right) tailward bursty bulk flows. From top to bottom, (first row) the superposed epoch analysis of H^+ perpendicular velocity (black solid line) (km/s). A black dotted line shows the parallel H^+ velocity. Gray lines show all the data used in the superposed epoch analysis. (second row) The same for O^+, using red lines for the superposed epoch results. (third row) The densities of H^+ (black) and O^+ (red) (cm^{-3}). (fourth row) The superposed epoch results for the magnetic field components with black for B_x, blue for B_y, and red for B_z (nT).

Criteria to identify bursty bulk flows based on the magnitude of the flow, similar to methods and criteria used by *Angelopoulos et al.* [1994], were tried, as well as criteria based on the perpendicular flow velocity by *Pitkänen et al.* [2013]. The results are similar, but the results using the magnitude of the flow in the $X_{GSM}-Y_{GSM}$ plane (V_{xy}) yield somewhat clearer results. Because the perpendicular velocity of the two ion species should be the same if the frozen-in condition holds, it is still more informative to study the perpendicular velocity. In this study, a BBF is thus defined using the perpendicular velocity: BBFs are periods with $V_{\perp xy} > 100$ km/s, with a peak within the structure of at least 200 km/s. Only BBFs within the plasma sheet as defined above are included. A three-data-point running mean was used on the data before the selection criteria were employed, so that single data points just below the velocity and plasma sheet thresholds would not affect the result.

3. Results

3.1. Superposed Epoch Study of Proton BBFs

BBF events in the plasma sheet fulfilling the definition given in section 2.2 were identified. Events were required to have at least five and at most 30 data points. The lower limit was set only to include clear events. The upper limit was to exclude possible other types of more continuous flows. In a final step the average velocity of the BBF event was compared to the average velocity in blocks of 30 data points before and after the BBF event. The BBF event was kept in the database only if the average velocity during the event was at

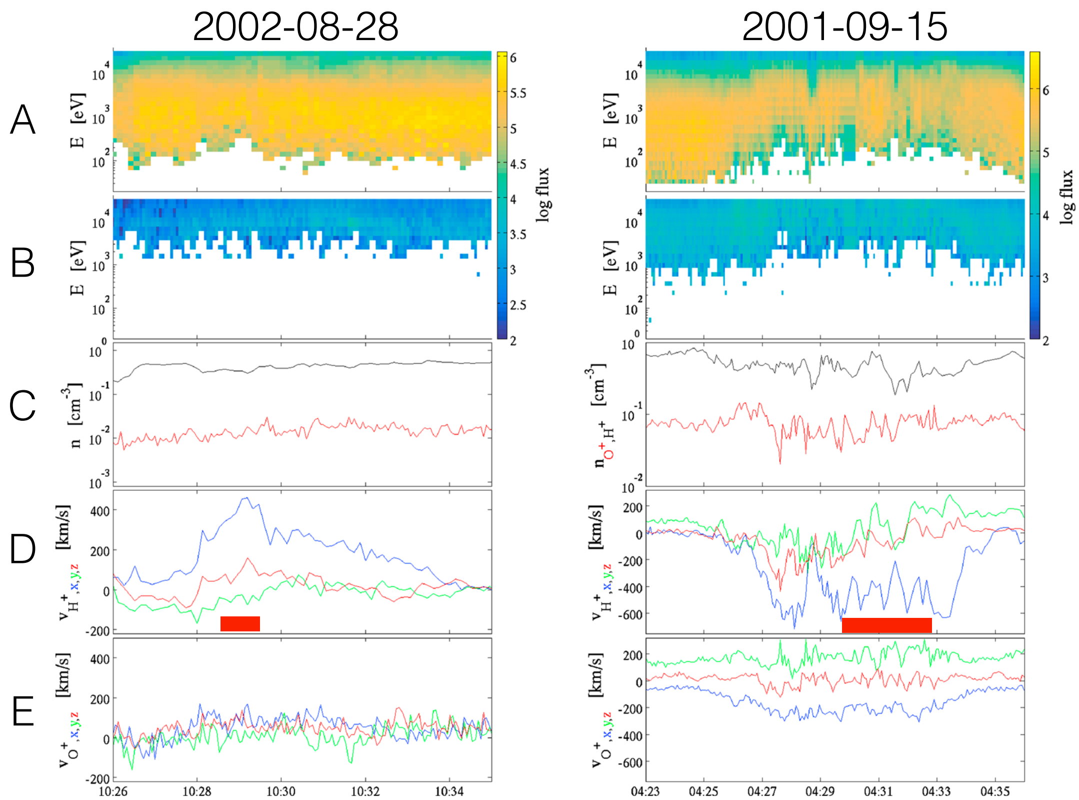

Figure 3. Sample data (left) from 2002-08-28 and (right) from 2001-09-15. (a) The energy spectrogram for H^+ ($\log_{10}$/cm^2/eV/sr/s); (b) the energy spectrogram for O^+ ($\log_{10}$/cm^2/eV/sr/s); (c) density (black line H^+, red line O^+) (cm^{-3}); (d) velocity components for H^+ and (e) velocity components for O^+, (km/s), where V_x is blue, V_y is green, and V_z is red. Red rectangles indicate times for the sample distribution functions shown in Figures 4 and 5.

least twice that of the time period before and after the event. This ensures that only isolated events, suitable for the superposed epoch study, are selected. The velocity profile used for the superposed epoch analysis consists of the BBF event and the two 30-data-point blocks observed before and after the BBF event. The BBF data were resampled on a 30-data-point grid, so the total superposed epoch events had a 90-data-point grid. This means a rescaling in time for short events. The idea is to get the average structure of the BBFs, with a consistent relation to the surrounding environment. The analysis was performed separately for earthward and tailward flow.

The result is shown in Figure 2. Data for earthward flow events are shown to the left, for tailward flow to the right. Figure 2 (first row) shows the H^+ $V_{\perp xy}$, positive in the X_{GSM} direction. Figure 2 (second row) shows the O^+ $V_{\perp xy}$ in the same format. All events used in the superposed epoch analysis are shown with gray lines, the superposed epoch result with a thick black line (H^+) or a thick red line (O^+). The parallel ion velocity is shown with a dotted line (positive earthward). Figure 2 (third row) shows the density of H^+ (black) and O^+ (red). The average densities are close to constant for both ion species. As the velocity increases, the particle flux is thus enhanced during the BBFs. The average densities show very little change for the earthward flow case, though a weak decrease can be discerned for H^+ during the BBF. There is a weak downward trend for the H^+ density during the BBF for tailward flow. These decreases are in accordance with the study by *Ohtani et al.* [2004], see, e.g., their Figures 3 and 7, respectively, as well as with the scenario of depleted flux tubes representing BBFs. The decreases have only a small effect on the particle fluxes. Generally, as the velocity increases, the particle flux is thus enhanced during the BBFs. Figure 2 (fourth row) shows the magnetic field components, with black for B_x, blue for B_y, and red for B_z. For earthward flow B_z is positive and increases during the BBF, while B_x shows a decreasing trend during the BBF. This is consistent with some degree of dipolarization during an earthward BBF. For tailward flow B_z is positive around the event, but negative in the middle of the event. Negative B_z is consistent with a location tailward but close to a reconnection site, i.e., in the earthward side of a plasmoid.

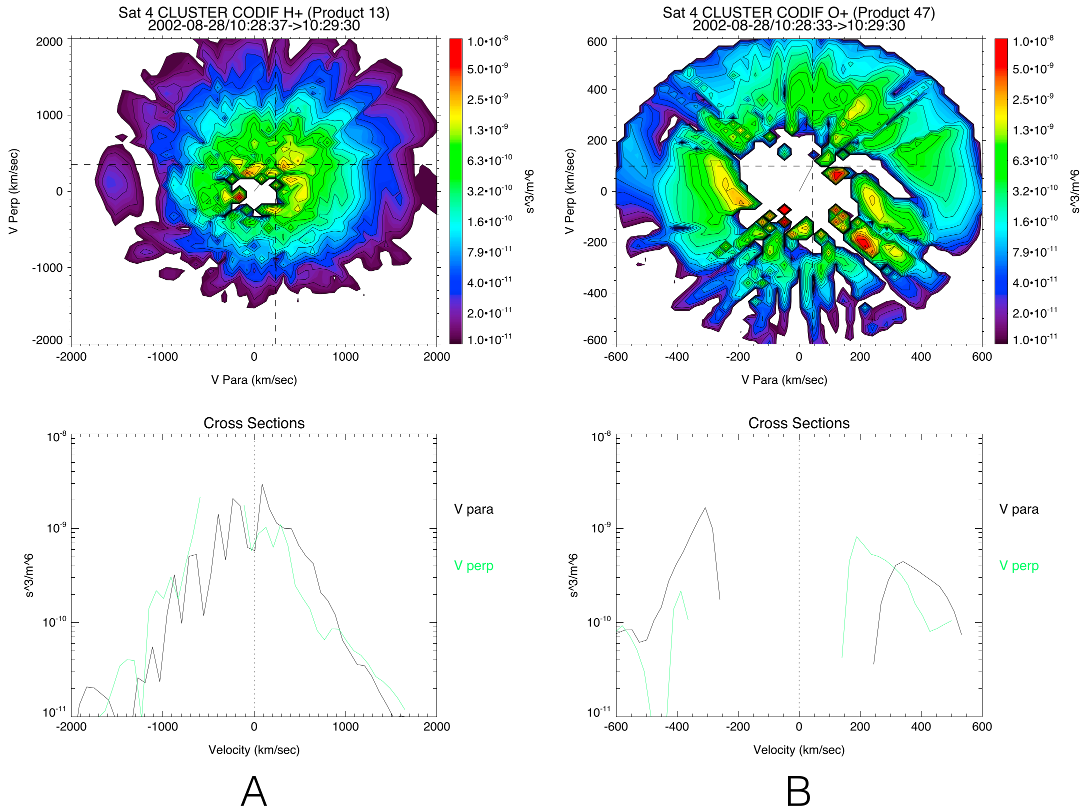

Figure 4. Velocity distribution functions for a sample earthward flow, (a) H$^+$ and (b) O$^+$ (s^3 m^{-6}). (top row) The distribution in magnetic field oriented coordinates, parallel component along X, perpendicular component (positive along the bulk perpendicular drift direction) along Y (km/s). Dashed lines intersect at the calculated bulk velocity. (bottom row) Cuts along the dashed lines.

For both earthward and tailward flows the O$^+$ ions do not reach anywhere near the velocity of the H$^+$ ions. There is a very weak enhancement of the average O$^+$ velocity for the earthward flow, about 70 km/s, but this is much smaller than the general variability of the velocity. For tailward flow the enhancement is larger, about 150 km/s. The O$^+$ density is significantly higher during periods of tailward flow as compared to earthward flow.

There is some enhancement of the parallel flow of H$^+$ during a BBF, but on average there is no enhancement of the parallel O$^+$ velocity.

3.2. Example Events

The superposed epoch study is complemented with two example events, one for earthward and one for tailward flow. Figure 3 (left) shows an example of earthward flow on 2002-08-28 and Figure 3 (right) an example of tailward flow from 2001-09-15, with, from top to bottom, energy spectrograms for H$^+$ (Figure 3a) and O$^+$ (Figure 3b), density for both ion species (Figure 3c), H$^+$ velocity components (Figure 3e), and finally, O$^+$ velocity components (Figure 3e). Red rectangles indicate the time periods for which sample distribution functions are shown in Figures 4 and 5.

The earthward flow sample is typical in the sense that not much response is seen in the O$^+$ velocity estimate when there is a clear increase in the H$^+$ velocity. The energy spectrograms of both ion species peak within the energy range of the instrument. The tailward flow case is typical in the sense that the velocity of the O$^+$ increase in a similar manner to the H$^+$ velocity, but with a lower magnitude. For this case it looks like the upper limit of the instrument energy range may be limiting the results.

Figure 4 shows the distribution functions for H$^+$ and O$^+$ for the earthward flow case on 2002-08-28, with a H$^+$ to the left and O$^+$ to the right. Figure 5 shows the same for the tailward case of 2001-09-15. The distributions confirms what could be discerned from the energy spectrograms: that the flux/distribution peaks within the instrument energy range for earthward flow as well as for tailward H$^+$ flow. For tailward O$^+$ flow,

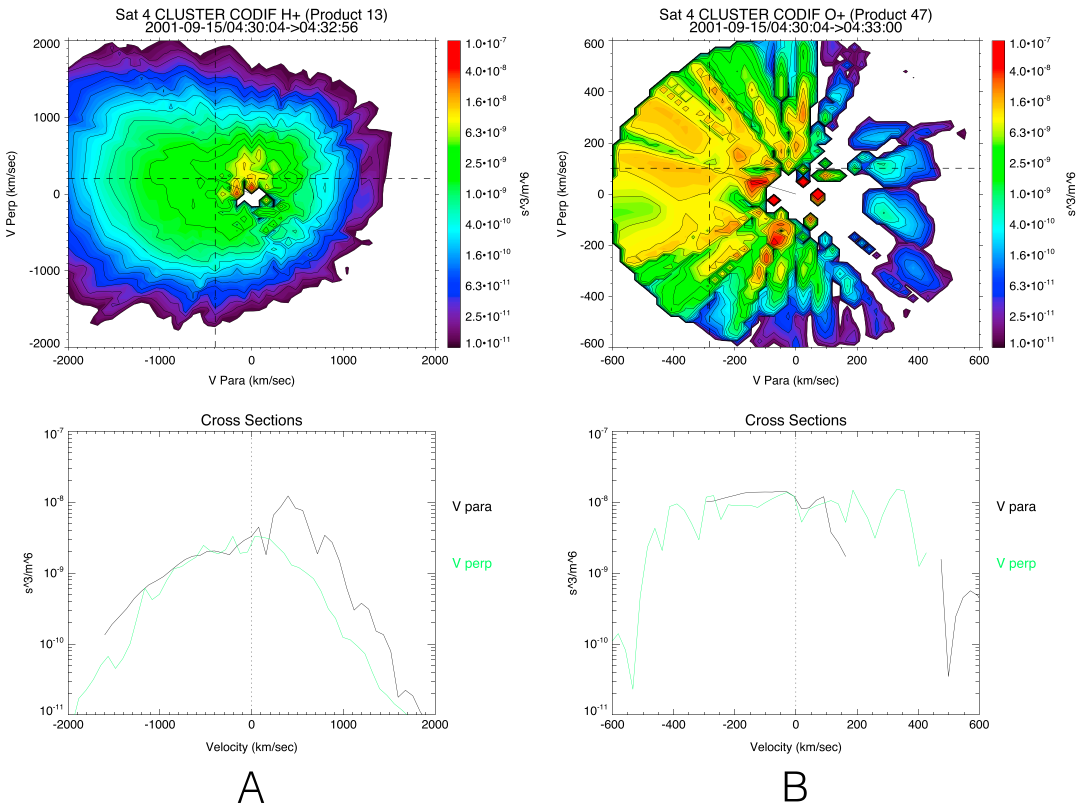

Figure 5. Velocity distribution functions for a sample tailward flow, (a) H^+ and (b) O^+ (s^3 m^{-6}). (top row) The distribution in magnetic field oriented coordinates, parallel component along *X*, perpendicular component (positive along the bulk perpendicular drift direction) along *Y* (km/s). Dashed lines intersect at the calculated bulk velocity. (bottom row) Cuts along the dashed lines.

the distributions are falling off somewhat toward higher energies, but it seems like the limited energy range is affecting the velocity estimate.

One may also note the lack of low-energy particles in the O^+ populations. These distributions may thus not be Maxwellian, and this may affect the results. The integrated moments still reflect the net motion of particles within the instrument energy range. The flux below about 1 keV is below the instrument one count level. The integrated counts and thus integrated flux in this energy range is thus negligible, and the total flux estimate is not much affected by the fluxes falling below the instrument sensitivity threshold below 1 keV. Thus, any low flux low-energy population should not much affect our moment estimates, though it may contribute to some underestimate of the velocity moment. One may note that the lowest 1 keV is a small part of the total energy range of the particle population for these sample distributions.

3.3. Correlation Between H^+ and O^+ Velocity

The superposed epoch analysis indicates a weak correlation between earthward H^+ and O^+ flow in BBFs and a somewhat higher correlation for tailward BBFs. Figure 6a shows the distribution of the O^+ velocity in the X_{GSM} direction as function of the H^+ velocity in the same direction, for all data fulfilling the plasma sheet criterion described in section 2.2. Each column of Figure 6 thus shows the normalized distribution of O^+ velocities for a given H^+ velocity bin.

Figure 6a (bottom) shows the logarithm of the number of data points that contributes to each bin. Low velocities dominate the distribution. Earthward flow dominates, in particular, for high velocities.

For negative (tailward) proton flow, there is a clear correlation between the flow of the two ion species for H^+ velocities from about −500 km/s to 0 km/s. The O^+ velocity is lower than the H^+ velocity by about a factor 2. For higher-magnitude H^+ tailward velocity the correlation breaks down, though the sign of the O^+ velocity is typically the same as that of the H^+ velocity. For positive H^+ velocity almost no correlation is seen. The O^+ velocity distribution is peaking at low positive values for all positive H^+ velocities. If one instead looks at the

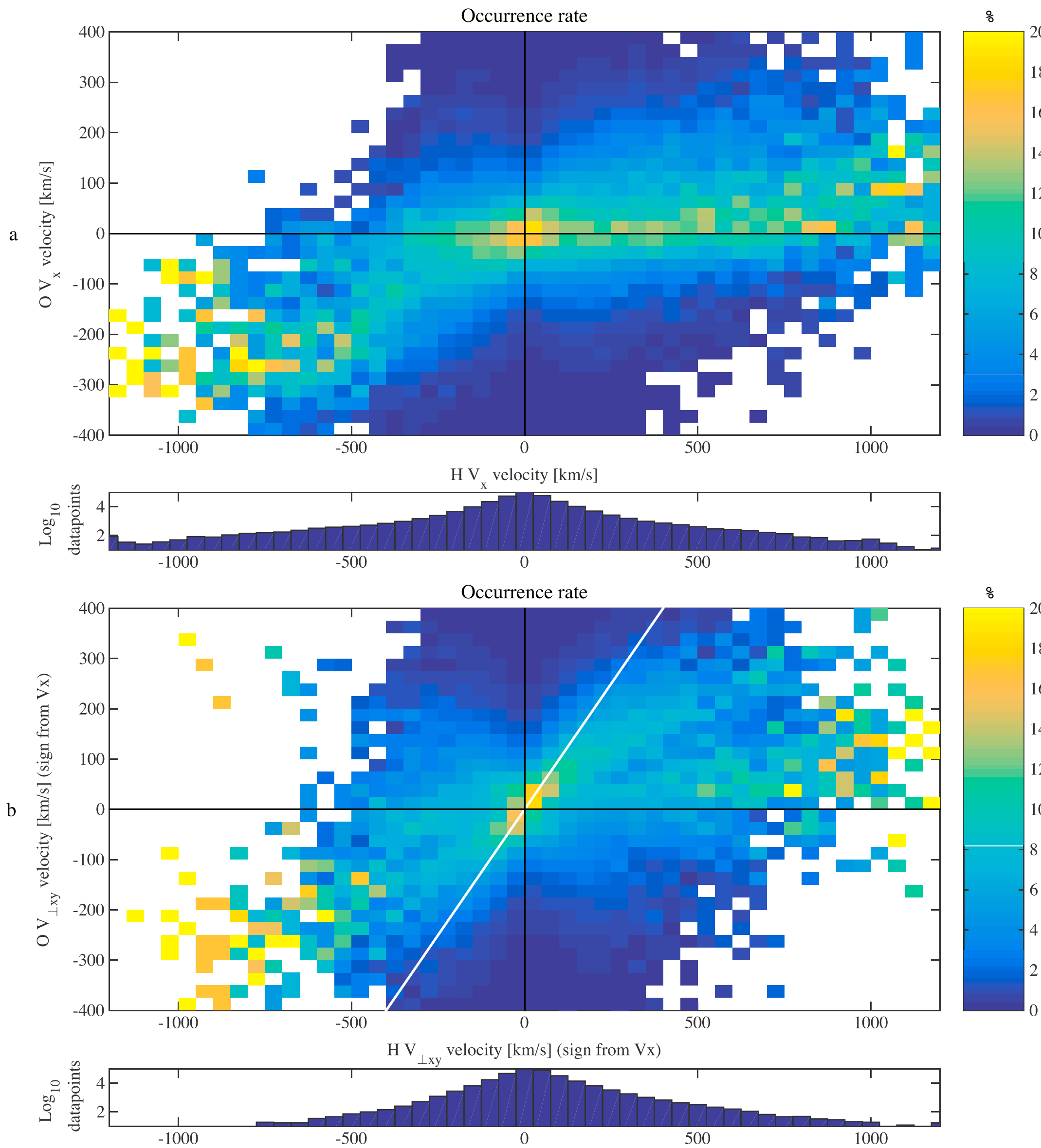

Figure 6. (a) Correlation between the H^+ (*X* axis) and O^+ (*Y* axis) earthward flow in the (top) X_{GSM} direction. (bottom) Logarithm of the number of data points contributing to each column. The color scale shows the occurrence frequency of the O^+ velocity for each interval of H^+ velocity. (b) The same for $V_{\perp xy}$. The white line indicates equal H^+ and O^+ velocity.

magnitude of v_{xy} a weak correlation between the velocity of the two ion species can be discerned also for positive H^+ velocities (not shown). The correlation is much further improved for the magnitude of $V_{\perp xy}$, as shown in Figure 6 b. The magnitudes of $V_{\perp xy}$ are similar in the range up to $\pm$100 km/s. The velocities are well correlated for velocities up to about $\pm$500 km/s, but the O^+ velocities are then lower than the H^+ velocities. This is consistent with the average response of the O^+ population at about 70 km/s for the H^+ BBFs. There is another peak in the O^+ velocity distribution at low positive values for all H^+ values, in particular, for positive H^+ velocities. This further strengthens the conclusion that the O^+ ions do not follow the H^+ convection in the plasma sheet.

In the data discussed above we showed the flow in the *X*-*Y* plane. Correlation between the perpendicular velocity is strongest when we compare the magnitudes of the velocities of the two ion species in this plane. This is because O^+ ions move more in the *Y* direction than H^+. We have calculated the average H^+ and O^+ velocity in the *X* and *Y* directions for time periods when the H^+ earthward velocity was above 100 km/s and

Table 1. Average Flow Velocities in the Plasma Sheet

	H^+ Earthward (km/s)	O^+ Earthward (km/s)	H^+ Duskward (km/s)	O^+ Duskward (km/s)
Average value	26	7.7	5.6	20
V_{H^+} >100 km/s	220	34	−1.6	28

the average for the whole data set. The result is summarized in Table 1. The O^+ motion is consistently more duskward than for H^+. For average O^+ velocities duskward motion dominates, whereas for H^+ the earthward velocity component always dominates.

The cross-tail electric field in the central plasma sheet is expected to have an average positive duskward component, consistent with transport toward the center of the plasma sheet and earthward. The higher duskward motion for O^+ as compared to the major ion species H^+ indicates a net motion of O^+ along the magnetotail electric field. This appears not to be related to BBFs in particular. This is consistent with a picture of magnetized H^+ and unmagnetized O^+.

4. Discussion

It has been shown in previous studies [e.g., *Angelopoulos et al.*, 1994] that BBFs contribute a significant fraction of the earthward transport of plasma in the plasma sheet. The superposed epoch study of this paper shows that O^+ does not follow along the H^+ ions in BBFs.

The correlation study shows that the most common O^+ earthward velocity for any given earthward H^+ velocity is a low positive value, a few 10 km/s, no matter how high the H^+ velocity. The correlation for perpendicular velocities is good only up to about 100 km/s, at higher velocities the O^+ ions lag behind. This means that the response of O^+ to disturbed conditions is fundamentally different from that of H^+. The earthward transport of O^+ is slower.

The main reason to expect that the H^+ and O^+ populations should have the same perpendicular bulk velocity in the tail is if the frozen-in condition holds. In such a case both species will $E \times B$ drift together.

In the cusp and mantle there is a tendency that H^+ and O^+ have the same bulk field-aligned velocity [*Nilsson et al.*, 2006, 2012], and the velocity filter effect yields further similar bulk velocities in the lobes [*Liao et al.*, 2012]. Thus, also the parallel velocities of the two ion species are likely to be the same as they enter an X line region in the plasma sheet. The superposed epoch study shows that we see no enhancement of the parallel flow of O^+ during BBFs defined from perpendicular flow of H^+. However, there is some corresponding enhancement of the parallel H^+ flow.

For flow from a small acceleration region (e.g., an X line), a velocity filter effect could also lead to similar velocities of ion populations observed at a significant distance from the source. On the other hand, *Karlsson et al.* [2015] showed that there is a consistently positive acceleration of ions in BBFs for tailward distances greater than 14 R_E; i.e., part of the acceleration cannot be considered to occur in a small region. Similarly, *Greco et al.* [2015] reported test particle simulations of how O^+ and H^+ were accelerated as a dipolarization front propagated through the tail. They found more acceleration of initially cold O^+, and a tendency for the bulk of the ions to be accelerated to about the same energy regardless of mass. Thus, the acceleration of O^+ close to an X line and at some distance when a dipolarization front passes through the plasma could be quite different. This is possibly what we see in our data, Figure 6b, where two peaks can be seen in the O^+ velocity distribution, in particular, for positive H^+ velocities. Tentatively, we have higher O^+ velocity/better correlation close to an X line. Then the situation is similar for earthward and tailward flows. As a dipolarization front passes through the plasma farther away from the X line, the typical response of O^+ is just a low earthward velocity.

A possible explanation for lower estimated O^+ velocities could be that a significant fraction of the O^+ ions are accelerated outside the instrument energy range. This would indeed frequently happen if the O^+ ions acquire the same velocity as the H^+ ions. The velocity correlation data shown in Figure 6 clearly show that this is not the case. The ion velocities start to differ at velocities well within the instrument energy range. Inspection of energy spectrograms (see our example cases) also show that we typically see the peak of the ion distribution

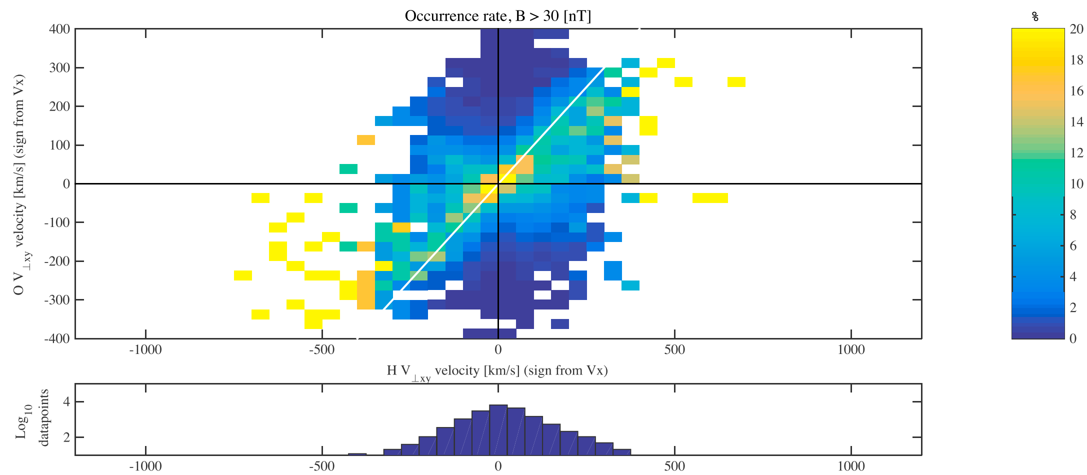

Figure 7. Correlation between the H^+ (X axis) and O^+ (Y axis) $V_{\perp xy}$ velocities for magnetic field strengths above 30 nT. The white line indicates equal H^+ and O^+ velocity.

within the instrument energy range. As there is still often a high-energy tail extending outside the instrument energy range, the calculated velocities are somewhat underestimated for the higher-velocity cases. Another concern is that the O^+ population falls below the one count sensitivity threshold below about 1 keV. This could lead to a slight overestimate of the velocity moments, but as this population below 1 keV does not contribute significantly to the total flux, it should have a rather small influence on the velocity estimates. Particles at energies below the instrument energy range is another matter, but as the drift energy corresponding to BBFs is well above the lower energy limit used of 40 eV, such a population is not likely and would anyway not affect our conclusions.

A higher correlation is observed between the perpendicular earthward ion flow of the two ion species (see Figure 6b). There is, however, a difference in the direction of the flow, with O^+ generally having a significantly stronger Y_{GSM} component of the flow (data not shown). The magnitude of $V_{\perp xy}$ is well correlated for earthward flow for velocities up to 500 km/s, but for velocities above about 100 km/s the O^+ velocity is significantly lower than the H^+ velocity. A duskward net motion for O^+ is seen. This is along the expected tail electric field direction and consistent with the O^+ ions not being frozen to the magnetic field. To further check this hypothesis about a demagnetization of the O^+ ions, we show in Figure 7 the same correlation plot as shown in Figure 6 b, but now for magnetic field strengths higher than 30 nT. We now, indeed, see a stronger similarity between the magnitudes of the velocities in the X-Y plane. The range of observed velocities is also much more restricted, only up to about 300 km/s.

For tailward plasma flow there is a much stronger correlation (see Figure 6a). Tailward high-speed streams are likely caused by reconnection close to Earth, which is more likely for disturbed conditions. For disturbed conditions the O^+ content of the plasma sheet is normally enhanced [*Kistler et al.*, 2006; *Maggiolo and Kistler*, 2014]. This is supported by the fact that the O^+ density is high for high-speed tailward flow, as shown in the superposed epoch analysis (Figure 2). The O^+ velocity is still lower than the H^+ velocity, but the correlation between the H^+ and O^+ velocity is significant, as opposite to the earthward flow case (Figure 6a).

Ohtani et al. [2015] also found an asymmetry between earthward and tailward flows. The O^+ to H^+ energy density decreased with increased earthward velocity, whereas it increased with increasing tailward velocity. This is consistent with the velocity correlation found in our study, where the bulk velocity increases for both ion species for tailward flow. *Ohtani et al.* [2015] also performed a superposed epoch analysis, but for a 30 min interval, compared to our 90 data points (6 min). They did not have composition data for the flow velocity but found that on this time scale both H^+ and O^+ energy density increased by about 20%. This is a much smaller change over a much longer time scale than the bulk velocity increases we have studied here.

Shay and Swisdak [2004] and *Liu et al.* [2015] described how the presence of two ion species can affect the reconnection process. In the case of one lighter and one heavier ion species (H^+, O^+) new length scales associated with the heavy ion whistler and Alfvén waves are established. The heavier ions are accelerated over larger length scales. In the *Shay and Swisdak* [2004] model the heavy and light ions end up at similar velocities over the larger-scale size. It seems possible that heavier ions attain a lower velocity if the dissipation region associated with the final acceleration of heavy ions is never established. This could be due to finite dimensions of the system. The geometry of the dissipation regions around an *X* line may also be asymmetrical, there being more room available on the tailward side, thus allowing for more acceleration of the heavier ion for the tailward flow case. Another possibility is that the O^+ fraction can often be significantly less than that in the *Shay and Swisdak* [2004] model, where the heavy ion density was assumed to be a fraction 0.64 of the light ion number density. If the minor ion population is too small, this could also lead to the fact that the larger scale regions, over which the heavier ions attain their full speed, are never established. The superposed epoch analysis indicated that the O^+ density was typically higher for the tailward BBFs. Similarly, the events reported by *Zong et al.* [2008] occurred for O^+-dominated conditions.

Liu et al. [2015] reported that O^+ was accelerated more in the *Y* direction than was H^+, consistent with the finding in our study that O^+ has a significant duskward component as compared to H^+. We however see this result on average, not just for high-speed flows.

The fact that we typically do not observe very high O^+ velocities indicate that the scale size of a region associated with the heavy ion Alfvén wave near a reconnection site is typically too small to provide acceleration of O^+ up to the velocity of H^+. The size of BBFs may lend support to this scenario. In some simulations the scale size of a BBF may be of the order of an O^+ gyroradius [*Ge et al.*, 2011]. In this study the average magnetic field for the superposed epoch study was 18 nT (not shown). For a typical plasma sheet energy of the order of 1 keV this means a gyroradius of the order of 1000 km. The gyroradius corresponding to an O^+ bulk drift of 400 km/s is about 1 R_E.

5. Conclusions

Simultaneous observations of H^+ and O^+ in the near-Earth plasma sheet were used to study the bulk velocities of the two ion species. Five clear points can be noted:

1. Only a modest increase in O^+ velocity is seen during earthward bursty bulk flows as identified from H^+ velocity data. This is true both for total earthward flow and perpendicular earthward flow in the $X_{GSM} - Y_{GSM}$ plane.
2. For earthward H^+ flow there is essentially no correlation between the velocities of H^+ and O^+ for all plasma sheet data, also outside BBFs. O^+ typically has a low earthward velocity regardless of the H^+ velocity.
3. The velocity perpendicular to the magnetic field of H^+ and O^+ in the near-Earth plasma sheet are similar up to values of about $\pm$100 km/s and correlated for H^+ velocities up to about 500 km/s. The O^+ velocity is significantly lower than that of H^+, and the O^+ flow is more in the $+Y_{GSM}$ direction than the H^+ flow.
4. The higher H^+ velocities indicate that H^+ is more efficiently accelerated in the process giving rise to BBFs. This may indicate that the scale size of the region associated with the heavy ion Alfvén wave around a reconnection site is typically too small to provide acceleration of O^+ up to the velocity of H^+. For tailward H^+ flow there is a significant correlation between the bulk velocities of H^+ and O^+, though the bulk velocity of O^+ is lower than that of H^+. Tailward flow in the plasma sheet is expected tailward of a reconnection region. The O^+ density is high for these events, consistent with them taking place for disturbed conditions. For Cluster observations of tailward flow, the observations must take place close to the reconnection site, which should increase the correlation between the velocities of the two ion species.
5. For tailward H^+ flow there is a clear correlation between the velocities of H^+ and O^+. The O^+ velocity is typically lower than the H^+ velocity. The higher correlation for tailward flow could be because observations are likely made closer to the reconnection site for tailward flow. A double peak in the distribution of the perpendicular O^+ flow for positive perpendicular H^+ flow may support this interpretation. When observations of earthward flow is made close to the reconnection site, the two ion velocities are correlated, giving rise to one of the observed peaks. At other locations the peak in the O^+ velocity distribution is at low positive values regardless of the H^+ velocity, tentatively corresponding to observations far from a reconnection site. Another possibility is that there is room for a larger region of O^+ acceleration on the tailward side of a reconnection site, which would enhance heavy ion acceleration and thus improve the correlation between H^+ and O^+ velocities.

Acknowledgments
H.G. was supported by the Belgian Science Policy Office through the Solar-Terrestrial Centre of Excellence and by PRODEX/Cluster contract 13127/98/NL/VJ(IC)-PEA 90316. H.N., M.H., and T.K. were supported by SNSB grant 78/11A and T.P. by SNSB grants 78/11B and 77/14. The data used can be freely retrieved from the Cluster Science Archive.

References

Angelopoulos, V., C. F. Kennel, F. V. Coroniti, R. Pellat, M. G. Kivelson, R. J. Walker, C. T. Russell, W. Baumjohann, W. C. Feldman, and J. T. Gosling (1994), Statistical characteristics of bursty bulk flow events, *J. Geophys. Res.*, *99*, 21,257–21,280, doi:10.1029/94JA01263.

Balogh, A., et al. (2001), The Cluster magnetic field investigation: Overview of in-flight performance and initial results, *Ann. Geophys.*, *19*, 1207–1217.

Dubouloz, N., M. Bouhram, C. Senior, D. Delcourt, M. Malingre, and J.-A. Sauvaud (2001), Spatial structure of the cusp/cleft ion fountain: A case study using a magnetic conjugacy between Interball AP and a pair of SuperDARN radars, *J. Geophys. Res.*, *106*, 261–274.

Escoubet, C. P., M. Fehringer, and M. Goldstein (2001), Introduction: The Cluster mission, *Ann. Geophys.*, *19*, 1197–1200.

Ge, Y. S., J. Raeder, V. Angelopoulos, M. L. Gilson, and A. Runov (2011), Interaction of dipolarization fronts within multiple bursty bulk flows in global MHD simulations of a substorm on 27 February 2009, *J. Geophys. Res.*, *116*, A00I23, doi:10.1029/2010JA015758.

Greco, A., A. Artemyev, and G. Zimbardo (2015), Heavy ion acceleration at dipolarization fronts in planetary magnetotails, *Geophys. Res. Lett.*, *42*, 8280–8287, doi:10.1002/2015GL066167.

Hamrin, M., P. Norqvist, O. Marghitu, S. Buchert, B. Klecker, L. M. Kistler, and I. Dandouras (2009), Occurrence and location of concentrated load and generator regions observed by Cluster in the plasma sheet, *Ann. Geophys.*, *27*, 4131–4146, doi:10.5194/angeo-27-4131-2009.

Hamrin, M., et al. (2014), Evidence for the braking of flow bursts as they propagate toward the Earth, *J. Geophys. Res. Space Physics*, *119*, 9004–9018, doi:10.1002/2014JA020285.

Karlsson, T., M. Hamrin, H. Nilsson, A. Kullen, and T. Pitkänen (2015), Magnetic forces associated with bursty bulk flows in Earth's magnetotail, *Geophys. Res. Lett.*, *42*, 3122–3128, doi:10.1002/2015GL063999.

Kistler, L. M., et al. (2005), Contribution of nonadiabatic ions to the cross-tail current in an O^+ dominated thin current sheet, *J. Geophys. Res.*, *110*, A06213, doi:10.1029/2004JA010653.

Kistler, L. M., et al. (2006), Ion composition and pressure changes in storm time and nonstorm substorms in the vicinity of the near-Earth neutral line, *J. Geophys. Res.*, *111*, A11222, doi:10.1029/2006JA011939.

Kistler, L. M., C. G. Mouikis, B. Klecker, and I. Dandouras (2010), Cusp as a source for oxygen in the plasma sheet during geomagnetic storms, *J. Geophys. Res.*, *115*, A03209, doi:10.1029/2009JA014838.

Kronberg, E. A., et al. (2014), Circulation of heavy ions and their dynamical effects in the magnetosphere: Recent observations and models, *Space Sci. Rev.*, *184*, 173–235, doi:10.1007/s11214-014-0104-0.

Liao, J., L. M. Kistler, C. G. Mouikis, B. Klecker, I. Dandouras, and J. C. Zhang (2010), Statistical study of O^+ transport from the cusp to the lobes with Cluster CODIF data, *J. Geophys. Res.*, *115*, A00J15, doi:10.1029/2010JA015613.

Liao, J., L. M. Kistler, C. G. Mouikis, B. Klecker, and I. Dandouras (2012), Solar cycle dependence of the cusp O^+ access to the near-Earth magnetotail, *J. Geophys. Res.*, *117*, A10220, doi:10.1029/2012JA017819.

Liu, Y. H., C. G. Mouikis, L. M. Kistler, S. Wang, V. Roytershteyn, and H. Karimabadi (2015), The heavy ion diffusion region in magnetic reconnection in the Earth's magnetotail, *J. Geophys. Res. Space Physics*, *120*, 3535–3551, doi:10.1002/2015JA020982.

Luo, H., E. A. Kronberg, E. E. Grigorenko, M. Fränz, P. W. Daly, G. X. Chen, A. M. Du, L. M. Kistler, and Y. Wei (2014), Evidence of strong energetic ion acceleration in the near-Earth magnetotail, *Geophys. Res. Lett.*, *41*, 3724–3730, doi:10.1002/2014GL060252.

Maggiolo, R., and L. M. Kistler (2014), Spatial variation in the plasma sheet composition: Dependence on geomagnetic and solar activity, *J. Geophys. Res. Space Physics*, *119*, 2836–2857, doi:10.1002/2013JA019517.

Mouikis, C. G, L. M. Kistler, Y. H. Liu, B. Klecker, A. Korth, and I. Dandouras (2010), H^+ and O^+ content of the plasma sheet at 15–19 Re as a function of geomagnetic and solar activity, *J. Geophys. Res.*, *115*, A00J16, doi:10.1029/2010JA015978.

Nilsson, H., et al. (2004), The structure of high altitude O^+ energization and outflow: A case study, *Ann. Geophys.*, *22*, 2497–2506.

Nilsson, H., et al. (2006), Characteristics of high altitude oxygen ion energization and outflow as observed by cluster: A statistical study, *Ann. Geophys.*, *24*, 1099–1112.

Nilsson, H., I. A. Barghouthi, R. Slapak, A. I. Eriksson, and M. André (2012), Hot and cold ion outflow: Spatial distribution of ion heating, *J. Geophys. Res.*, *117*, A11201, doi:10.1029/2012JA017974.

Ohtani, S., M. Nosé, Y. Miyashita, and A. T. Y. Lui (2015), Responses of different ion species to fast plasma flows and local dipolarization in the plasma sheet, *J. Geophys. Res. Space Physics*, *120*, 187–200, doi:10.1002/2014JA020517.

Ohtani, S.-I., M. A. Shay, and T. Mukai (2004), Temporal structure of the fast convective flow in the plasma sheet: Comparison between observations and two-fluid simulations, *J. Geophys. Res.*, *109*, A03210, doi:10.1029/2003JA010002.

Pitkänen, T., M. Hamrin, P. Norqvist, T. Karlsson, and H. Nilsson (2013), IMF dependence of the azimuthal direction of earthward magnetotail fast flows, *Geophys. Res. Lett.*, *40*, 5598–5604, doi:10.1002/2013GL058136.

Rème, H., et al. (2001), First multispacecraft ion measurements in and near the Earth's magnetosphere with the identical Cluster ion spectrometry (CIS) experiment, *Ann. Geophys.*, *19*, 1303–1354.

Seki, K., R. C. Elphic, M. Hirahara, T. Terasawa, and T. Mukai (2001), On atmospheric loss of oxygen ions from Earth through magnetospheric processes, *Science*, *291*, 1939–1941.

Shay, M. A., and M. Swisdak (2004), Three-species collisionless reconnection: Effect of O^+ on magnetotail reconnection, *Phys. Rev. Lett.*, *93*(17), 175001, doi:10.1103/PhysRevLett.93.175001.

Slapak, R., H. Nilsson, and L. G. Westerberg (2013), A statistical study on O^+ flux in the dayside magnetosheath, *Ann. Geophys.*, *31*, 1005–1010.

Zong, Q.-G., et al. (1998), Energetic oxygen ion bursts in the distant magnetotail as a product of intense substorms: Three case studies, *J. Geophys. Res.*, *103*, 20,339–20,364, doi:10.1029/97JA01146.

Zong, Q.-G., H. Zhang, S. Y. Fu, Y. F. Wang, A. Korth, P. W. Daly, and T. A. Fritz (2008), Ionospheric oxygen ions dominant bursty bulk flows: Cluster and Double Star observations, *J. Geophys. Res.*, *113*, A07S23, doi:10.1029/2007JA012764.